Data-Driven Support Vector Machine to Predict Thin-Walled Tube Energy Absorbers Behavior

Ghasemi, Mostafa; Silani, Mohammad; Yaghoubi, Vahid; Concli, Franco

DOI
10.1007/978-3-031-38274-1_54

Publication date
2023

Document Version
Final published version

Published in
Towards a Smart, Resilient and Sustainable Industry - Proceedings of the 2nd International Symposium on Industrial Engineering and Automation ISIEA 2023

Data-Driven Support Vector Machine to Predict Thin-Walled Tube Energy Absorbers Behavior

Mostafa Ghasemi[1], Mohammad Silani[1,2](✉), Vahid Yaghoubi[3], and Franco Concli[2]

[1] Department of Mechanical Engineering, Isfahan University of Technology, 84156-83111 Isfahan, Iran
mohammad.silani@unibz.it

[2] Facoltà di Scienze e Tecnologie, Libera Università di Bolzano/Bozen, Piazza Università, 1, 39100 Bolzano, Italy

[3] Structural Integrity and Composites, Faculty of Aerospace Engineering, Delft University of Technology, 2629 HS Delft, The Netherlands

Abstract. To design a more efficient energy absorber, it is critical to evaluate how changing the design parameters affects its performance, and also determine each one's order of significance. In this paper, using a new approach, the behavior and response of straight, double-tapered, and triple-tapered thin-walled tubes with rectangular cross sections under axial and dynamic loading are investigated by performing a sensitivity analysis on a support vector machine (SVM) as a surrogate machine learning model. First, a finite element model of the energy absorber is constructed and validated with available experimental and theoretical studies. Next, a design of experiments was developed using the Sobol series sampling method and an appropriate dataset was created. This information is then used to develop an SVM model to predict the initial peak load and mean load of tubes. The accuracy of the machine learning created in this study is then assessed, and it is demonstrated that the developed model can precisely predict the performance of the absorber. The machine learning model is then subjected to a Sobol sensitivity analysis, and the outcomes are compared to those of the parametric study. The results suggest that the thickness of the tube has a stronger effect on the absorber performance than other geometric parameters. Comparing the effects of different material parameters on the behavior of tubes, the results show that yield strength has the greatest impact on the response of the energy absorber. It is also observed that the tapered tubes have a much lower initial peak load compared to straight ones.

Keywords: Thin-walled tube · Energy absorber · Finite element · Machine learning · SVM · Surrogate model · Sensitivity analysis

1 Introduction

Recent innovations in crashworthiness studies enable the development of safe vehicle designs that dissipate the most crash energy through material deformation. The different deformation modes of the structural elements acting during the crash are often

Y. Borgianni et al. (Eds.): ISIEA 2023, LNNS 745, pp. 642–654, 2023.
https://doi.org/10.1007/978-3-031-38274-1_54

what determine this energy-absorbing capacity of the structure [1]. The employment of complicated high-fidelity FEM to mimic the response of mechanical components under impact loads is motivated by the complexity that arises during theoretical analysis and high-cost experimental investigations [2, 3]. The energy absorber transforms kinetic energy into a different kind of energy that can either be irreversible (like plastic strain energy) or reversible (like elastic strain energy) [4]. Different energy absorbers have been designed depending on the use and application. Due to their availability, low cost, optimal performance under dynamic loads, and high efficiency, thin-walled tube energy absorbers are widely used in different industries [5]. Thin-walled energy absorbers can have one or more oblique faces. Since the tapered thin-walled energy absorbers have more stable and desirable performance under oblique and normal loads, they are typically more desirable compare to the straight tubes [6].

Reid et al. [7] used experimental findings of the axial loading of rectangular tubes under quasi-static and dynamic conditions to investigate the stability and energy-absorbing properties of foam-filled and foam-empty tubes of various densities. They also provided a straightforward theoretical model to describe how foam and metal tubes interact. Reid and Reddy [6] investigated how tapered thin-walled tubes responded to dynamic and quasi-static inclined loads. Their findings demonstrated that tapered tubes are desirable to straight tubes because they are significantly less susceptible to global buckling and can absorb energy in an oblique orientation. To analyze the impact of adding foam to thin-walled tubes, Mirfendereski et al. [5] proposed a finite element model and investigate the effects of foam density, the oblique sides, and boundary conditions on the crushing behavior of rectangular-section tubes using a parametric research. This parametric study investigated the load-displacement curve, specific energy absorption, fold length, and deformation mode of foam-filled tubes with respect to input parameters.

Several experimental and numerical studies in this area have been conducted recently in addition to pioneering efforts. For instance, Zhigang et al. [8] tested the capacity of magnesium and aluminum circular thin-walled tubes to absorb energy. They came to the conclusion that the energy-absorbing mechanism in aluminum tubes is mostly controlled by plastic yielding and folding, whereas it is primarily controlled by fracture in magnesium tubes. To increase crashworthiness, Jiang et al. [9] suggested a thin-walled square tube that was filled with hollow aluminum metal spheres. They investigated crashworthiness and deformation mechanisms using various stacking modes using experimental and numerical simulations. They also conducted some parametric experiments, which demonstrated that the size, wall thickness, and stacking modes of the hollow spheres are the most important factors in crashworthiness.

A machine learning-based optimization strategy for energy-absorbing structures was presented by Li et al. [10]. Their approach, in contrast to the conventional optimization method, may eliminate the undesirable deformations for energy-absorbing structures. Ghasemi et al. presented a machine learning model to predict the energy absorbing performance of tapered thin-walled tubes [11]. This work was focused only on the triple-tapered thin-walled tubes. The least-squares boosting algorithm was used in this study and the validity and accuracy of the model were also investigated.

The goal of this study is to propose a new approach to investigate the thin-walled tube's absorbing performance using a surrogate machine learning model-based sensitivity analysis. The benefit of such a model is that it gives us the capability of having infinite and limitless access to the absorber's performance in the design space without being concerned about the high-fidelity finite element simulation's time-consuming restrictions and its computing costs. To do so, a finite element model is first created and verified. The impact of different input parameters on the initial peak and mean loads is then investigated using parametric analysis. Next and using Python scripting capability in Abaqus, a script is built to simulate the tube energy absorbers and build a dataset while taking into account an acceptable Design Of Experiment (DOE) based on the Sobol series sampling approach. Next, a machine-learning model was trained using this data set, and the performance of the trained model was evaluated. Finally, the machine-learned model is subjected to a sensitivity analysis using Sobol's sensitivity indices.

2 Finite Element Model and the Verification

2.1 Description of FE Model

To build the numerical model of the tube energy absorber in Abaqus [12], a similar approach to [11] was used. The same reported input parameters were utilized to compare the results to those of Mirfendereski et al. [5] (10° tapered angle, 1.5 mm thickness, 300 mm height, $100 \times 50\,\text{mm}^2$ cross-section). The tube was crushed between two rigid flat plates with mass of 90 kg and impact speed of 15 m/s that were placed on its top and bottom [5]. The material of the tube is mild steel with 304.6 MPa yield strength, 205 GPa Young's modulus, 0.3 Poisson's ratio and $7700\,\text{kg/m}^3$ density. To incorporate the strain rate effect on the constitutive equation of the material, the Cowper-Symonds (C.S.) equation was used here with the material constants of $D = 6844\,\text{s}^{-1}$ and $q = 3.91$ [6, 7, 13].

The geometry was discretized using the shell element type (S4R), and the appropriate element size of $3 \times 3\,\text{mm}^2$ was determined using a mesh convergence study. Using symmetric boundary conditions, only half of the model was simulated. The energy-absorbing process was modeled using the explicit dynamic technique. This approach is particularly effective to simulate post-buckling. The deformation mode of the tube during straight external loading is shown in Fig. 1.

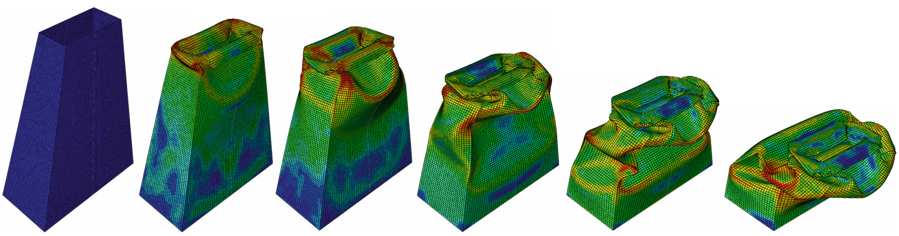

Fig. 1. The deformation mode of the thin-walled energy absorber during straight loading.

2.2 Finite Element Model Verification

To verify the numerical model, the load results of this simulations were compared to those of Mirfendereski et al. [5]. Here, the same geometry and dimensions, material model and boundary conditions were used to make the comparison possible. To have a quantitative comparison, the initial peak and mean loads of both studies at 200 mm deflection were tabulated in Table 1 which show a maximum difference of 3% and 0.1% in the initial peak and mean loads, respectively.

To also verify the results of the straight tube, the same methodology was repeated for a straight tube with the same geometrical and material inputs as before, but without any tapered wall. The results are tabulated in Table 2 which shows a difference of 6.38% and 9.29% in the initial peak and mean loads with [14], respectively.

Nagel and Thambiratnam's paper is considered to be a pioneer work in using FEM to study thin-walled tube energy absorbers' behavior and has been the basis of many following studies. Mirfendereski et al. used the same consideration as Nagel et al. to develop a finite element model and reported the results for the triple-inclined thin-walled tubes as well. Hence, these two studies were chosen to be a criterion to assess the current finite element model's validation.

Table 1. Load comparison between the current study and Mirfendereski et al. [5] for the tapered tube.

Load (kN)	Mirfendereski et al.	Current simulations	Difference (%)
Initial peak load	170	165.17	2.84
Mean load	46	45.95	0.11

Table 2. Load comparison between the current study and Nagel and Thambiratnam [14] for the straight tube.

Load (kN)	Nagel and Thambiratnam	Current simulations	Difference (%)
Initial peak load	200	187.24	6.38
Mean load	45	49.18	9.29

3 Input Parameter Selection and Design of Experiments (DOE)

To have an effective design of experiments, the input parameters should be recognized first. Here, two sets of geometrical and material inputs are considered. The thickness, taper angle, and cross-sectional ratio are the geometrical input parameters. The limits of these parameters are tabulated in Table 3 [5, 14, 15]. It should be noted that the section's width is considered to be constant (50 mm according to [16, 17]) and only section's length controls the cross-sectional ratio.

Table 3. The current study's geometrical parameter range

Cross-sectional ratio	Tube thickness (mm)	Taper angle (°)
[1, 2]	[1, 2.5]	(0, 20]

Here we have different material parameters which should be considered in the DOE. First, the C.S. material constants for six materials were taken out from the available studies and tabulated in Table 4. The other material constants of these materials like elastic constants, plastic constants, and density are also extracted and listed in Table 5. Here we suppose that the materials behave fully plastic in the plastic region resulting to fewer input parameters and improved machine-learning accuracy.

Table 4. Material constants for Cowper-Symonds equation

Coefficient	Mild steel [6]	High-tensile steel AH32 [18]	Stainless steel 304L [19]	Stainless steel S30408 [20]	Stainless steel S31608 [20]	Aluminum alloy 6063 - T6 [21]
$D(s^{-1})$	6844	3200	3000	996.1	1195.7	6500
q	3.91	5	2.8	3.456	5.222	4

The final eight parameters that have been determined as the uncertain input parameters are shown in Table 6. Utilizing the Sobol series sampling approach, 200 points are selected from the parameter space to form the dataset at which the FE model will be assessed. Furthermore, it's obvious that the taper angle is not involved in the straight tube's uncertain parameters, and this specific tube has seven input parameters. The outputs of the ML model were the initial peak and mean loads, respectively.

Table 5. Mechanical properties of materials considered in this study

Property	Mild steel [14]	High-tensile steel AH32 [22]	Stainless steel 304L [22]	Stainless steel S30408 [20]	Stainless steel S31608 [20]	Aluminum alloy 6063 - T6 [23]
Young' modulus (GPa)	205	196	200.2	196	190	69
Poisson's ratio	0.3	0.3	0.3	0.3	0.3	0.33
Yield Strength (MPa)	304.6	357.35	309.48	298.46	267.38	225.78
Density (gr/cm^3)	7.7	7.8	8.0	8.0	8.0	2.7

Table 6. The statistical distribution of uncertain geometrical and material inputs

Parameter	Definition (unit)	Distribution type	Mean	Standard deviation
t	Thickness (mm)	Uniform	1.75	0.433
csr	Cross-sectional ratio	Uniform	1.5	0.289
α	Taper angle (degree)	Uniform	10.0	5.774
ρ	Density (gr/cm^3)	Log-normal	1.888	0.439
E	Young's modulus (GPa)	Log-normal	5.11	0.43
σ_Y	Yield strength (MPa)	Log-normal	5.673	0.155
D	C.S. constant, multiplier (s^{-1})	Log-normal	7.946	0.815
q	C.S. constant, exponent	Log-normal	1.38	0.232

4 The Tube Energy Absorber Performance: A Parametric Study

The parametric study in this section examines how different input factors affect the behavior of tube energy absorbers. A tube energy absorber should typically have a greater mean load and a minor initial peak load [14]. To have a reference for the input parameters, the tube thickness, tube cross-sectional ratio, tube taper angle, and material were set to 1.5 mm, 2.0, 10°, and mild steel, respectively. It's obvious that the taper angle is not included in the straight tube's parameters.

4.1 Tube Thickness's Effect on the Tube Performance

The tube thickness's effect on the initial peak and mean loads is illustrated in Fig. 2. It is quite clear from the figure that for all tubes, increasing the tube thickness results in an increase in the initial peak load and mean load. For example, the peak load and the mean load in the triple tapered thin-walled tube with a variation of thickness from 1 mm to 2.5 mm increase about 3 and 4 times, showing the dominant effect of thickness on the energy absorbers. Although the tapered and straight thin-walled tube absorbers have almost the same mean loads, the tapered tubes have a much lower initial peak load which is a favorable behavior for tapered tubes (e.g., in the thickness of 1.5 mm, the initial peak load of the tripled tube and the double tube is about 17% and 36% lower than the straight tube).

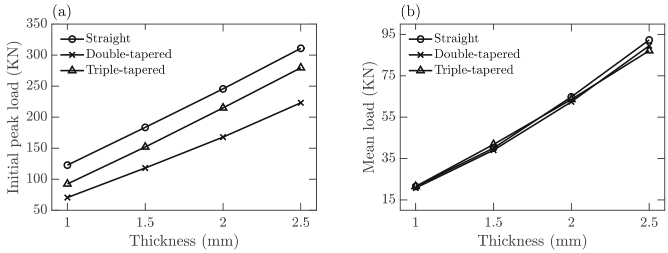

Fig. 2. (a) The initial peak load's variation versus thickness, (b) the mean load's variation versus thickness.

4.2 Cross-Sectional Ratio's Effect on the Tube Performance

The cross-sectional ratio's effect on the initial peak and mean loads is depicted in Fig. 3. The figure shows that when the cross-sectional ratio increases, the initial peak load increases, but the mean load does not change significantly. For example, for a triple-tapered tube, by increasing this ratio from 1 to 2, the value of the initial peak load increases by approximately 84%, while the mean load increases by about 18%. It is clear in Fig. 3(a) that the tapered tubes have a lower initial peak load compared to the straight tube. It is also clear that the thickness's effect on the initial peak and mean loads is more evident than the cross-sectional ratio's effect. It is noteworthy that in this study, only the effect of the cross-sectional ratio between 1 and 2 was investigated. Suppose the behavior of the absorber is investigated in a wider range of cross-sectional ratios. In that case, this parameter could have more significant effects on the amount of absorbed energy by the absorber.

4.3 Taper Angle's Effect on the Tube Performance

Taper's angle effect on the tube behavior is shown in Fig. 4. Moving from the straight state (zero-degree tapered angle) to the tapered state, Fig. 4(a) shows a 30% reduction of initial peak load. Figure 4(b) shows the effect of the taper angle on the mean load,

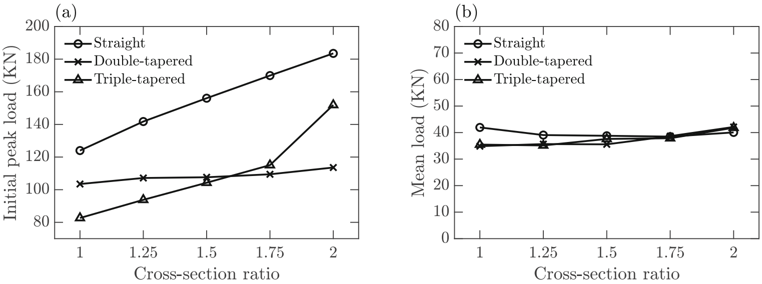

Fig. 3. (a) The initial peak load's variation versus cross-sectional ratios, (b) the mean load's variation versus cross-sectional ratios.

which points out that the taper angle greater than zero does not significantly affect the load value. As the slope increases, the mean load increases by about 16% in the tripled taper tube and remains almost constant in double-tapered tubes.

In a nutshell, when the tube is moving from the straight state to the tapered state, the amount of the peak load of the tube absorber changes suddenly, which demonstrates the importance of the taper angle on the behavior of the tube absorber in this region (the mean load does not undergo much change). After this region, the taper angle has a smaller effect on the tube absorber behavior compared to the thickness and cross-sectional ratio (the maximum initial peak load and mean load changes in tripled taper tube with a change of taper angle from 5 to 20° are about 15% and 16%, respectively). Also, it is clear that the primary peak load of the inclined double-sided loop is less than that of the inclined three-sided loop, and on the contrary, the mean load of the inclined three-sided absorber is more in these shapes.

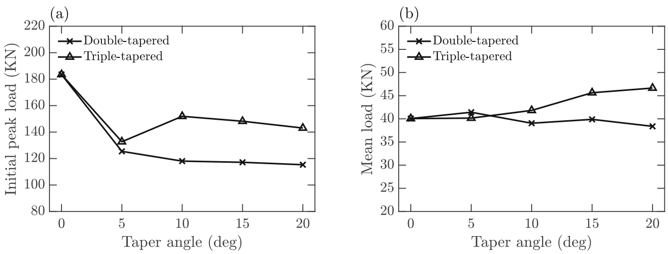

Fig. 4. (a) The initial peak load's variation versus taper angle, (b) the mean load's variation versus taper angle.

4.4 Material Effects on the Tube Performance

The material effects on the initial peak and mean loads are illustrated in Fig. 5 (the order of materials in these two figures is based on the tube absorber mean load). In all types of absorbers, aluminum alloy shows the minimum initial peak and mean loads. Besides, for the mean load, it can be claimed that materials with higher yield strength show a higher mean load. For example, in all three kinds of absorbers, the high-resistance steel alloy AH32 absorber with the highest yield strength has the highest mean load. Except for alloyS31608, the same prediction is valid for the initial peak load. Noteworthy, apart from the geometrical characteristics considered the same for all materials, the rest of the material parameters of these materials, including density, yield strength, Young's modulus, and strain rate relationship constants, are different from each other. For this reason, the difference in the behavior of these absorbers cannot be attributed to only one specific parameter. Nevertheless, the relatively high impact of the yield strength on the performance of the tube energy absorber is evident.

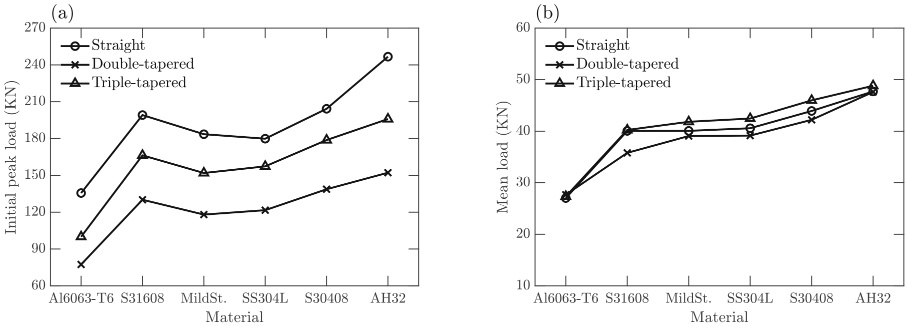

Fig. 5. (a) The variation of the initial peak load versus material, (b) the variation of the mean load versus material.

Figure 5 also shows that the number of tapered sides in the tube absorber affects the overall behavior of the tube energy absorber. The straight energy absorber has the highest initial peak load, followed by the triple-tapered tube and then the double-tapered tube, which shows the lowest initial peak load. It can also be concluded that the mean loads of different energy absorbers are close together.

5 Machine Learning Algorithm

It is desirable to replace the FE model with a regression model since assessing the FE model takes a lot of time. The regression model will then be utilized for sensitivity analysis. For speed comparison, on average, each finite element simulation of a tube impact test takes about 30 min, while each machine learning model prediction of absorber performance takes about 0.2 ms. The quickness of this surrogate model offers a great opportunity to cover almost the entire design space in sensitivity analysis and be assured its result is reliable and converged perfectly. The next step is to choose the right model. Consequently, the support vector machine with a third-order polynomial kernel function, which is called Cubic-SVM, is selected in this study. The proposed method is accurate and has enough robustness to the outliers [24]. The command "fitrsvm" was used to train a regression model on the data set in MATLAB's Machine Learning toolbox. To do so, 120 (60% of the dataset) and 80 (40% of the dataset) samples are used to train and test the model, respectively.

5.1 Model Validation

Evaluation of the performance and accuracy of learned models is essential. The trained model's validity and accuracy are assessed in this section. Two different criteria were used: Normalized Mean Squared Error (NMSE) and correlation coefficient (R):

$$NMSE = \frac{\frac{1}{n}\sum_{i=1}^{n}(x_i - y_i)^2}{\frac{1}{n}\sum_{i=1}^{n}x_i^2} \tag{1}$$

$$R = \frac{\sum_{i=1}^{n}(x_i - \overline{x})(y_i - \overline{y})}{\sqrt{\sum_{i=1}^{n}(x_i - \overline{x})^2 \sum_{i=1}^{n}(y_i - \overline{y})^2}} \tag{2}$$

where x_i, y_i and n are actual values of the output parameter, predicted values, and the number of data points, respectively. Also, the bar sign upon each symbol indicates the mean of the values of that parameter (desired values of R and NMSE are 1 and 0, respectively).

Figure 6(a) and (b) show a comparison between the ML predicted values and the finite element ones, containing the best-fitted linear regression line. The slope of the regression line is close to the unity which shows the validity of the machine learning model.

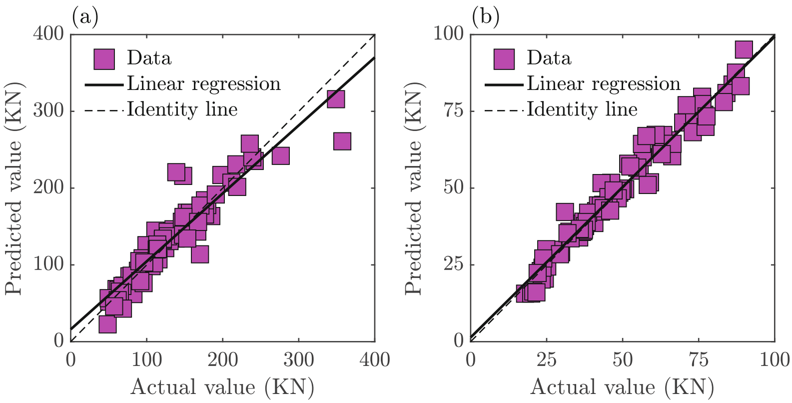

Fig. 6. The finite element and ML predictions including linear regression analysis for (a) initial peak load, and (b) for the mean load.

The simulation dataset has been split up randomly 50 times into train and test datasets, to offer a statistic on the performance of the regression model. A model was trained for each dataset, and then its performance was evaluated using R and NMSE, and the results are summarized in Table 7. The correlation coefficient (R) was found to be close to 1. Also, the NMSE values are close to zero in both cases, proving the effectiveness and accuracy of the developed machine learning models.

Table 7. The mean and standard deviation (SD) for validation measures on the test dataset

Type of energy absorber	Initial peak load				Mean load			
	R		NMSE		R		NMSE	
	Mean	SD	Mean	SD	Mean	SD	Mean	SD
Straight	0.9838	0.0051	0.003	0.0009	0.9902	0.0023	0.0028	0.0006
Double-tapered	0.9147	0.0231	0.0178	0.0048	0.986	0.0032	0.0036	0.0008
Triple-tapered	0.923	0.0165	0.0212	0.0065	0.9805	0.0047	0.0051	0.0013

5.2 Sensitivity Analysis

Additionally, a Sobol sensitivity analysis was conducted to look into how input factors affected outcomes. For this, the UQLab plugin [25] was employed. The outcomes of this study for the first peak and mean loads are displayed in Fig. 7. It can be concluded that the tube thickness has the strongest effect on the initial peak and mean loads.

Also, yield strength is the second effective parameter for the mean load. Regarding the initial peak load, it can be seen that after the thickness, most of the input parameters are involved in the peak load of the absorber. Still, the stronger relative influence of the yield strength after the thickness can be seen. In addition, the effect of the cross-sectional

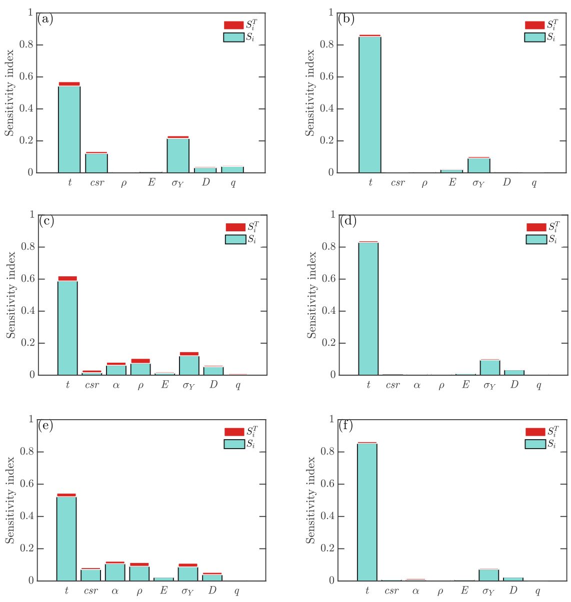

Fig. 7. Sobol's sensitivity indices (first-order and the total indices) of (a) for the straight tube's initial peak load, (b) for the straight tube's mean load, (c) for double-tapered tube's initial peak load, (d) for the double-tapered tube's the mean load, (e) for triple-tapered tube's initial peak load, (f) for the triple-tapered tube's the mean load.

ratio on the initial peak load of straight (Fig. 7(a)) and tripled taper absorbers (Fig. 7(c)) is greater compared to the double tapered absorber (Fig. 7(c)), which is also depicted in Fig. 3(a). These results are a validation for the parametric studies' findings.

6 Conclusion

This paper presents and validates a numerical model to predict thin-walled energy absorber tubes' behaviors based on FEM. To investigate the effects of input parameters on the outputs (initial peak and mean loads), an appropriate parametric study was performed. The results of the parametric study show that tube thickness and yield strength are the most effective geometrical and material parameters on the tube performance, respectively. Next, based on an appropriate DOE, a machine-learned model was trained and tested to predict the thin-walled tubes' performances. R and NMSE criteria were used to examine the model's validity and accuracy. It was established that the suggested machine-learned model is accurate, reliable, and effective for the design and performance assessment of energy absorbers. The machine-learned model was then subjected to a Sobol sensitivity analysis. Finally, it is worth noting that in this research only the axial dynamic loading was the case and changes in loading conditions were not included. As a further attempt, one can involve loading variables as well, e.g. loading direction (axial or oblique), crash speed, and lower rigid plate's mass, and evaluate their impact on the absorber's performance.

Acknowledgment. M. Silani would like to thank the financial support of "*Provincia Autonoma di Bolzano/Alto Adige –Ripartizione Innovazione, Ricerca, Universita e Musei*".

References

1. Concli, F., Maccioni, L.: Experimental-numerical calibration of the fracture locus of a weathering steel. WIT Trans. Eng. Sci. **124**, 219–227 (2019)
2. Concli, F., Gilioli, A.: Numerical and experimental assessment of the mechanical properties of 3D printed 18-Ni300 steel trabecular structures produced by selective laser melting–a lean design approach. Virtual Phys. Prototyp. **14**(3), 267–276 (2019)
3. Concli, F., Gilioli, A.: Numerical and experimental assessment of the static behavior of 3D printed reticular Al structures produced by selective laser melting: progressive damage and failure. Procedia Struct. Integr. **12**, 204–212 (2018)
4. Alghamdi, A.A.A.: Collapsible impact energy absorbers: an overview. Thin-walled Struct. **39**(2), 189–213 (2001)
5. Mirfendereski, L., Salimi, M., Ziaei-Rad, S.: Parametric study and numerical analysis of empty and foam-filled thin-walled tubes under static and dynamic loadings. Int. J. Mech. Sci. **50**(6), 1042–1057 (2008)
6. Reid, S.R., Reddy, T.Y.: Static and dynamic crushing of tapered sheet metal tubes of rectangular cross-section. Int. J. Mech. Sci. **28**(9), 623–637 (1986)
7. Reid, S.R., Reddy, T.Y., Gray, M.D.: Static and dynamic axial crushing of foam-filled sheet metal tubes. Int. J. Mech. Sci. **28**(5), 295–322 (1986)

8. Li, Z.Z., et al.: Experimental study on the crush behavior and energy-absorption ability of circular magnesium thin-walled tubes and the comparison with aluminum tubes. Thin-Walled Struct. **163**, 114492 (2021)
9. Jiang, B., Chen, X., Yu, J., Zhao, Y., Xie, Z., Tan, H.: Energy-absorbing properties of thin-walled square tubes filled with hollow spheres. Thin-Walled Struct. **180**, 109765 (2022)
10. Li, Z., Ma, W., Yao, S., Xu, P., Hou, L., Deng, G.: A machine learning based optimization method towards removing undesired deformation of energy-absorbing structures. Struct. Multidiscip. Optim. **64**(2), 919–934 (2021). https://doi.org/10.1007/s00158-021-02896-1
11. Ghasemi, M., Silani, M., Yaghoubi, V., Concli, F.: Performance prediction of thin-walled tube energy absorbers using machine learning. In: Managing and Implementing the Digital Transformation: Proceedings of the 1st International Symposium on Industrial Engineering and Automation ISIEA 2022, pp. 87–99 (2022)
12. ABAQUS/Explicit User's Manual Version 6.4 (2004)
13. Wierzbicki, T., Abramowicz, W.: On the crushing mechanics of thin-walled structures. J. Appl. Mech. Trans. ASME **50**(4), 727–734 (1983)
14. Nagel, G.M., Thambiratnam, D.P.: A numerical study on the impact response and energy absorption of tapered thin-walled tubes. Int. J. Mech. Sci. **46**(2), 201–216 (2004)
15. Shariatpanahi, M., Masoumi, A., Ataei, A.: Optimum design of partially tapered rectangular thin-walled tubes in axial crushing. Proc. Inst. Mech. Eng. Part B J. Eng. Manuf. **222**(2), 285–291 (2008)
16. Abramowicz, W., Jones, N.: Dynamic axial crushing of circular tubes, vol. 2, no. 3, pp. 263–281 (1984)
17. Liu, Y.: Design optimisation of tapered thin-walled square tubes, vol. 13, no. 5, pp. 543–550 (2008)
18. Paik, J.K., Thayamballi, A.K.: Ultimate Limit State Design of Steel-Plated Structures. Wiley, Hoboken (2003)
19. Forrestal, M.J., Sagartz, M.J.: Elastic–plastic response of 304 stainless steel beams to impulse loads (1978)
20. Jia, S., Tan, Q., Ye, J., Zhu, Z., Jiang, Z.: Experiments on dynamic mechanical properties of austenitic stainless steel S30408 and S31608. J. Constr. Steel Res. **179**, 106556 (2021)
21. Bodner, S.R., Symonds, P.S.: Experimental and theoretical investigation of the plastic deformation of cantilever beams subjected to impulsive loading (1962)
22. Paik, J.K., Kim, K.J., Lee, J.H., Jung, B.G., Kim, S.J.: Test database of the mechanical properties of mild, high-tensile and stainless steel and aluminium alloy associated with cold temperatures and strain rates. Ships Offshore Struct. **12**(sup1), S230–S256 (2017)
23. Hsu, S.S., Jones, N.: Dynamic axial crushing of aluminium alloy 6063 - T6 circular tubes. Lat. Am. J. Solids Struct. **1**(3), 277–296 (2004)
24. Cortes, C., Vapnik, V.: Support-vector networks. Mach. Learn. **20**(3), 273–297 (1995)
25. Marelli, S., Sudret, B.: UQLab: a framework for uncertainty quantification in Matlab. In: Vulnerability, Uncertainty, and Risk: Quantification, Mitigation, and Management, pp. 2554–2563 (2014)